Metal–Organic Frameworks

DOI: 10.1002/ange.200702324

Crystal Structure and Guest Uptake of a Mesoporous Metal–Organic Framework Containing Cages of 3.9 and 4.7 nm in Diameter**

*Young Kwan Park, Sang Beom Choi, Hyunuk Kim, Kimoon Kim, Byoung-Ho Won, Kihang Choi, Jung-Sik Choi, Wha-Seung Ahn, Nayoun Won, Sungjee Kim, Dong Hyun Jung, Seung-Hoon Choi, Ghyung-Hwa Kim, Sun-Shin Cha, Young Ho Jhon, Jin Kuk Yang, and Jaheon Kim**

Porous crystalline solids with a regular array of well-defined pores have proved to be very useful in gas storage, sensing, separation, optics, nanoreactors, and catalysis.[1] Although metal–organic frameworks (MOFs) have greatly expanded the scope of porous materials, especially in terms of chirality,[2] materials design,[3] and very high surface areas,[4] they are largely restricted to the microporous regime. While numerous inorganic porous solids such as silicates and carbons exist with a wide range of pore sizes at the micro- to mesoscales, few MOFs with mesopores have been reported.[5] Therefore, it is a great challenge to synthesize robust mesoporous MOFs, especially those with pore sizes greater than 3 nm in diameter. Equally challenging is the task of characterizing their structures at atomic resolution, because the structural details of such frameworks are usually sacrificed as the pore size increases.[6] Herein, we report the crystal structure, permanent porosity, and luminescence properties of a mesoporous MOF (**1**), the framework of which is composed of fused 3.9- and 4.7-nm cages.

Mesoporous MOF **1** was prepared as truncated-octahedral crystals by a solvothermal reaction between triazine-1,3,5-tribenzoic acid (H_3TATB) and $Tb(NO_3)_3{\cdot}5H_2O$ in a mixture of *N*,*N*-dimethylacetamide (DMA), methanol, and water at 105 °C for 2 days (Figure 1 a; see the Supporting Information). Single-crystal X-ray diffraction data were collected up to 1.13-Å resolution in a face-centered cubic unit cell at the beamline facilities designed for macromolec-

[*] Y. K. Park, S. B. Choi, Dr. Y. H. Jhon, Prof. J. K. Yang, Prof. J. Kim
Department of Chemistry, Soongsil University
Seoul 156-743 (Korea)
Fax: (+82) 2-824-4383
E-mail: jaheon@ssu.ac.kr
H. Kim, Prof. K. Kim
National Creative Research Center for Smart Supramolecules and Department of Chemistry, Pohang University of Science and Technology, Pohang 790-784 (Korea)
B.-H. Won, Prof. K. Choi
Department of Chemistry, Korea University, Seoul 136-704 (Korea)
J.-S. Choi, Prof. W.-S. Ahn
Department of Chemical Engineering, Inha University
Incheon 420-751 (Korea)
N. Won, Prof. S. Kim
Department of Chemistry, Pohang University of Science and Technology, Pohang 790-784 (Korea)
Dr. D. H. Jung, Dr. S.-H. Choi
Insilicotech Co. Ltd., Kolontripolis A-1101
Seongnam 463-805 (Korea)
G.-H. Kim, Dr. S.-S. Cha
Beamline Division, Pohang Accelerator Laboratory
Pohang 790–784 (Korea)

[**] This work was supported by the Hydrogen Energy R&D Center (J.K.), the Carbon Dioxide Reduction and Sequestration R&D Center (W-S.A.), the 21st Century Frontier R&D Program funded by the Ministry of Science and Technology of Korea, the Creative Research Initiatives and BK 21 Programs (K.K.), and a Korean Research Foundation Grant funded by the Korean Government (MOEHRD; KRF-2005-005J13102; S.K.). We thank Prof. Ji Man Kim (Department of Chemistry, Sung Kyun Kwan University) for the SAXS measurements. The X-ray diffraction experiments were performed at the Pohang Accelerator Laboratory (beamlines 4A and 6B) supported by MOST and Pohang University of Science and Technology.

Supporting information for this article is available on the WWW under http://www.angewandte.org or from the author.

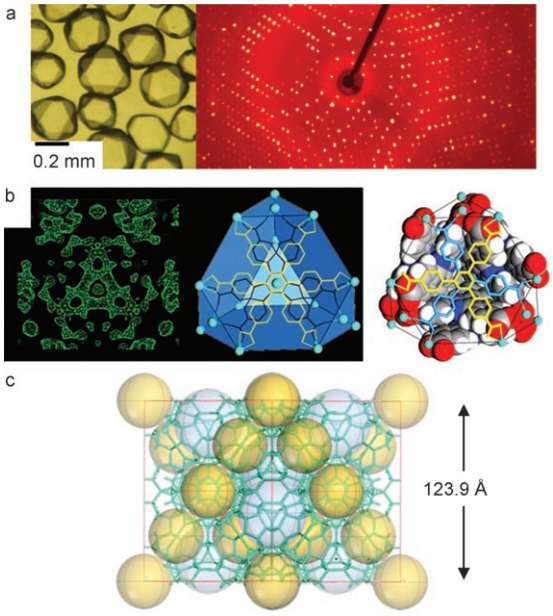

Figure 1. a) Single crystals of **1** (left), and a sampled X-ray diffraction pattern one such crystal (right). b) A three-dimensional electron-density map of a face of a truncated ST (left), and its corresponding disordered (middle) and ordered (right) structural models. C gray, H white, N blue, O red (space-filling model); outer (yellow) and inner (blue) TATB ligands shown as stick models. The Tb^{3+} ions (light blue spheres) sit on the triangular faces of a truncated ST. c) A cubic unit cell viewed along the [101] direction. The large and small spheres represent the inner spaces of the mesocages, and the sticks connect the Tb^{3+} ions that are the vertices of the truncated STs.

ular crystallography at Pohang Accelerator Laboratory (PAL). The crystal structure shows that a total of 1088 Tb^{3+} ions, or 272 Tb_4 cluster units, are distributed in the unit cell (Figure 1c; see the Supporting Information).[7] Each Tb_4 unit has a trigonal-planar geometry with an average interatomic distance of 5.14 Å between the peripheral atoms and the central atom. The separation between two peripheral Tb^{3+} ions is about 8.82 Å. In turn, four Tb_4 moieties form a tetrahedral arrangement, or a supertetrahedron (ST), with a separation of about 16.27 Å between the central Tb^{3+} ions. In the unit cell, 68 of these unique truncated STs are fused together, producing 17 additional truncated STs and making a three-dimensional extended network. The truncated ST can be regarded as a structural subunit of **1** (Figure 1b). The three-dimensional extended network built by the Tb^{3+} ions is similar to those of MIL-100 and MIL-101, which exhibit the MTN zeotype.[5b,c]

The metal ions and ligands in **1** are assembled in a very unique way to produce the zeotype network. Owing to the large separation between the Tb^{3+} ions (5.14 Å) compared to the usual separation between carboxylate-bridged lanthanide ions (ca. 4 Å),[8] the pair of TATB ligands on each face of the truncated ST link nine Tb^{3+} ions in a very delicate way; the outer TATB ligand joins three peripheral Tb^{3+} ions in a bidentate fashion, while the inner TATB ligand binds three central Tb^{3+} ions and another three peripheral Tb^{3+} ions in a bi-monodentate fashion (Figure 1b and the Supporting Information). This coordination mode makes the central Tb^{3+} ions of the trigonal-planar Tb_4 moieties and the four internal TATB ligands almost unexposed to the pore. Two TATB ligands stack with each other on each hexagonal face of the truncated ST, such that the central triazine rings are superimposed and the benzoate moieties are staggered. Therefore, the truncated ST becomes thicker and heavier, owing to the double coats. Crystallographic mirror planes bisect all the independent truncated STs, causing the TATB ligands to disorder over two sets of sites about the mirror planes (Figure 1c and the Supporting Information).

Above and below the trigonal-planar Tb_4 moieties in each truncated ST, a total of 12 TATB ligands are bound. The TATB ligands link each truncated ST to four adjacent truncated STs. Two truncated STs are linked in an eclipsed fashion, despite having the possibility of adopting a gauche geometry.[9] The fusion of the building blocks produces five- and six-membered rings in the framework, which, considering van der Waals radii, have free diameters of 13.0 and 17.0 Å, respectively (Figure 2a and the Supporting Information). These openings are the windows of two kinds of large cages, the shapes of which are slightly distorted spheres. The smaller cage **S** is surrounded by 20 truncated STs and has 12 pentagonal windows (Figure 2c). Its internal free diameter is 39.1 Å. The larger cage **L**, defined by 28 truncated STs and having 12 pentagonal and 4 hexagonal windows, has an internal free diameter of 47.1 Å (Figure 2c). The hexagonal windows are tetrahedrally located in an **L** cage, and through these windows all the **L** cages are fused together to form a diamond-like network. The **S** cages are fused to the **L** cages by sharing pentagonal windows and also form a diamond-like net, if the centers of four **S** cages joined together are considered

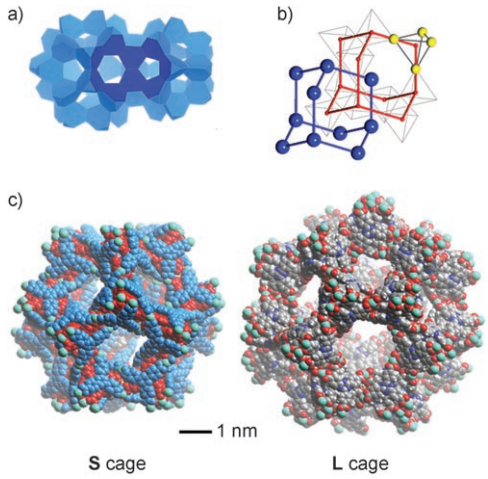

Figure 2. a) The network of fused **S** and **L** mesocages formed by the truncated STs. b) The doubly interpenetrating diamond-like net formed by the **L** cages (blue spheres) and the centers (small red spheres) of tetrahedra of **S** cages (yellow spheres). c) The **S** and **L** mesocages drawn as space-filling models. In the **S** cage, the inner TATB ligands are drawn in red, and outer ligand in blue; in the **L** cage, the atoms are drawn in their atomic colors. C gray, H white, N blue, O red, Tb light blue.

(Figure 2b). On the basis of the crystal-structure analysis, the repeating unit was chosen to be $\{Tb_{16}(TATB)_{16}\}$ with $Z = 68$, and by other chemical analyses, including elemental analyses, the compound was formulated as $[Tb_{16}(TATB)_{16}(DMA)_{24}]\cdot(DMA)_{91}(H_2O)_{108}$. Thermogravimetric analysis (TGA) of the as-prepared crystals at ambient atmosphere showed three weight-loss steps corresponding to the removal of the free guests (47% at 120°C), the coordinating ligands (9% at 320°C), and the TATB ligands with decomposition (30% at 520°C; see the Supporting Information). It was virtually impossible to clearly define the free guests inside the pores with the current X-ray data, owing to the severe disorder common to microporous MOFs.[4]

A nitrogen adsorption measurement on the evacuated as-prepared crystals at 77 K and up to 760 Torr showed a nearly reversible isotherm (Figure 3a). This sorption behavior is different from that of other similar mesoporous MOFs, such as MIL-100 and MIL-101, in terms of the number of steps and their distinctness.[5b,c] If it is assumed that the steps at 200 and 300 Torr are due to the **S** and **L** pores, respectively, the isotherm more or less resembles the isotherm found for calcined MCM-41, for which the pore-filling mechanism is still not absolutely clear.[10] The Brunauer–Emmett–Teller (BET) surface area was calculated as 1419 $m^2 g$, and the Langmuir surface area calculated with the amount of adsorbed nitrogen and the molecular area of N_2 (16.2 $Å^2$) was estimated as 2887 $m^2 g$.

When the samples were activated at 160°C, the surface-area values increased to 1783 $m^2 g$ (BET) and 3855 $m^2 g$ (Langmuir), with retention of the original sorption behavior (Figure 3a). This change in the surface area was also confirmed by CO_2 adsorption measurements at ambient temperature (Figure 3b). The as-prepared sample could store 14 $mmol g^{-1}$ (ca. 43 bar), which increased to

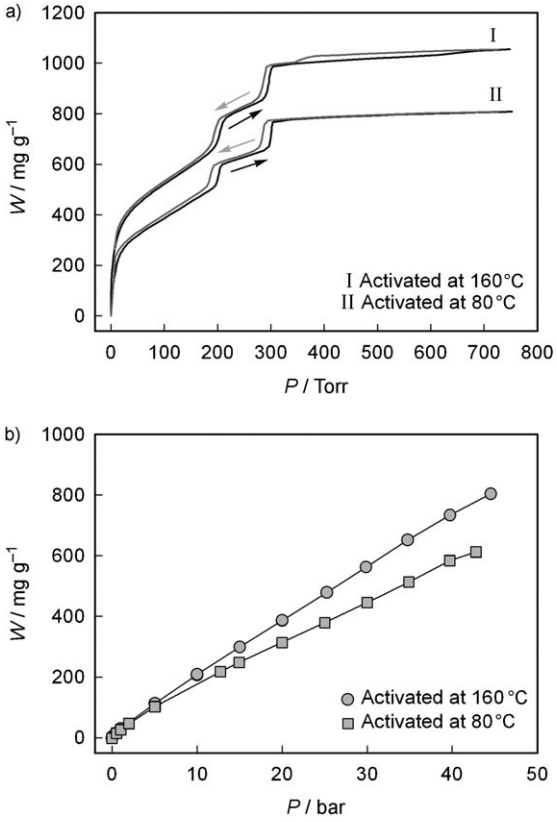

Figure 3. a) Nitrogen sorption isotherms at 77 K for samples of **1** activated at 80 °C and 160 °C, respectively. b) High-pressure carbon dioxide adsorption isotherms at ambient temperature for the same samples used in (a).

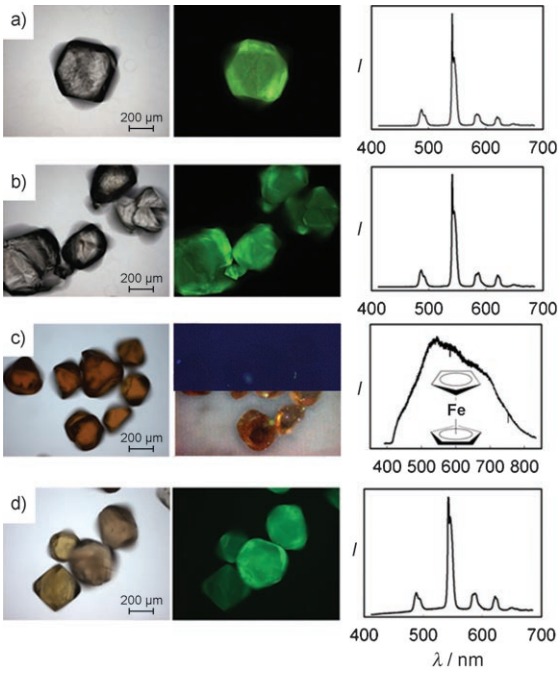

Figure 4. a) Microscope images of a crystal of **1** taken in transmission mode (left) and in fluorescence mode (middle), and its luminescence spectrum (right). b) As in (a), for a bulk sample. c) As in (a), for ferrocene-containing crystals. In the fluorescence image, half of the background color was subtracted to show the crystals. d) As in (a), for the crystals used in (c) after evacuation at 50 °C for 1 day.

18 mmol g^{-1} (ca. 45 bar) for the activated sample. These values are located between the uptakes of MOF-177 and of zeolite 13X.[11] The unsaturated uptake values of **1** indicate that most of the pore space is not filled with CO_2 molecules.

The as-prepared crystals of **1** emit strong green light at 488, 541, 584, and 620 nm (Figure 4a), which is very similar to that emitted by other Tb^{3+}-containing MOFs with very different framework structures.[8a,b] The emission spectrum of a single crystal was identical to that of the bulk (Figure 4b). As the host framework has both a high thermal stability and sufficient rigidity under vacuum, ferrocene guest molecules could be included by a sublimation procedure at 100 °C.[12] The crystal color changed to dark brown, and ^{1}H NMR spectra and elemental analyses suggested that at least 65 ferrocene molecules per formula unit, which is equivalent to 4420 ferrocene molecules per unit cell, were included in the pores of **1** (see the Supporting Information). For the ferrocene-containing crystals, no strong green emission was observed; instead, a weak and broad emission from the included ferrocene molecules appeared (Figure 4c). As the ferrocene molecule absorbs light at wavelengths that overlap with the emission region of the framework of **1**,[13] it is likely that an efficient energy transfer from the host framework to the ferrocene molecules occurs. The crystal of **1** appears to act as an antenna harvesting photons for the included ferrocene molecules, because the emission from the host–guest system is actually stronger than that from the ferrocene molecules alone, though the mechanism of the energy transfer requires further investigation (see the Supporting Information).

It is interesting to note that the included ferrocene molecules could be released under vacuum at an elevated temperature, and that afterwards the green emission from the crystal of **1** was recovered completely. Moreover, the spectrum exactly matched that of the evacuated host crystals, and the ferrocene emission disappeared (Figure 4d).

This work demonstrates that mesoporous MOFs with pores of at least 4.7 nm in diameter can be synthesized and that their crystal structures can be directly determined at atomic resolution by X-ray crystallography, without assuming the building-block structures as in previous cases.[5b,c] Moreover, the experimental observations on **1** also support that host frameworks built with coordination linkages can be robust enough to tolerate a mesoscale void space. These results are believed to be valuable for the exploration of mesoporous MOFs, into which a variety of functionality can be introduced as for their microporous relatives.

Received: May 26, 2007
Published online: August 7, 2007

Keywords: adsorption · luminescence · mesoporous materials · metal–organic frameworks · terbium

[1] *Handbook of Porous Solids* (Eds.: F. Schüth, K. S. W. Sing, J. Weitkamp), Wiley-VCH, Weinheim, **2002**.

[2] a) J.-S. Seo, D. Whang, H. Lee, S. I. Jun, J. Oh, Y. J. Jeon, K. Kim, *Nature* **2000**, *404*, 982 – 986; b) D. Bradshaw, J. B. Claridge, E. J. Cussen, T. J. Prior, M. J. Rosseinsky, *Acc. Chem. Res.* **2005**, *38*, 273 – 282.

[3] a) B. Moulton, M. J. Zaworotko, *Chem. Rev.* **2001**, *101*, 1629 – 1658; b) O. M. Yaghi, M. O'Keeffe, N. Ockwig, H. K. Chae, M. Eddaoudi, J. Kim, *Nature* **2003**, *423*, 705 – 714.

[4] a) H. Li, M. Eddaoudi, M. O'Keeffe, O. M. Yaghi, *Nature* **1999**, *402*, 276 – 279; b) H. Chae, D. Y. Siberio-Pérez, J. Kim, Y. Go, M. Eddaoudi, A. Matzger, M. O'Keeffe, O. M. Yaghi, *Nature* **2004**, *427*, 523 – 527.

[5] a) M. Eddaoudi, J. Kim, N. Rosi, D. Vodak, M. O'Keeffe, O. M. Yaghi, *Science* **2002**, *295*, 469 – 472; b) G. Férey, C. Serre, C. Mellot-Draznieks, F. Millange, S. Surblé, J. Dutour, I. Margiolaki, *Angew. Chem.* **2004**, *116*, 6456 – 6461; *Angew. Chem. Int. Ed.* **2004**, *43*, 6296 – 6301; c) G. Férey, C. Mellot-Draznieks, C. Serre, F. Millange, J. Dutour, S. Surblé, I. Margiolaki, *Science* **2005**, *309*, 2040 – 2042; d) X.-S. Wang, S. Ma, D. Sun, S. Parkin, H.-C. Zhou, *J. Am. Chem. Soc.* **2006**, *128*, 16474 – 16475.

[6] a) Y. Sakamoto, M. Kaneda, O. Terasaki, D. Y. Zhao, J. M. Kim, G. Stucky, H. J. Shin, R. Ryoo, *Nature* **2000**, *408*, 449 – 453; b) L. A. Solovyov, A. N. Shmakov, V. I. Zaikovskii, S. H. Joo, R. Ryoo, *Carbon* **2002**, *40*, 2477 – 2481; c) L. A. Solovyov, V. I. Zaikovskii, A. N. Shmakov, O. V. Belousov, R. Ryoo, *J. Phys. Chem. B* **2002**, *106*, 12198 – 12202; d) S. Inagaki, S. Guan, T. Ohsuna, O. Terasaki, *Nature* **2002**, *416*, 304 – 307; e) S. Che, A. E. Garcia-Bennett, T. Yokoi, K. Sakamoto, H. Kunieda, O. Terasaki, T. Tatsumi, *Nat. Mater.* **2003**, *2*, 801 – 805; f) Y. Sakamoto, T.-W. Kim, R. Ryoo, O. Terasaki, *Angew. Chem.* **2004**, *116*, 5343 – 5346; *Angew. Chem. Int. Ed.* **2004**, *43*, 5231 – 5234.

[7] Crystal data for **1**: $C_{384}H_{192}N_{48}O_{96}Tb_{16}$, $M_r = 9556.58$, cubic, space group $F\bar{4}3m$ (No. 216), $a = 123.901(1)$ Å, $V = 1902061(27)$ Å^3, $Z = 68$, $d_{calcd} = 0.567$ g cm^{-3} for the framework only, $T = 90(2)$ K, crystal size $0.35 \times 0.35 \times 0.35$ mm^3, $\lambda = 0.89999$ Å, $2\theta = 46.84°$, 1358 parameters, $R1 = 0.2074$ ($I > 2\sigma(I)$, 29225 reflections), $wR2 = 0.4932$ (all data, 30902 reflections), GOF = 1.101. See details in the Supporting Information. CCDC-648613 contains the supplementary crystallographic data for this paper. These data can be obtained free of charge from The Cambridge Crystallographic Data Centre via www.ccdc.cam.ac.uk/data_request/cif.

[8] a) T. M. Reineke, M. Eddaoudi, M. Fehr, D. Kelley, O. M. Yaghi, *J. Am. Chem. Soc.* **1999**, *121*, 1651 – 1657; b) H.-T. Zhang, Y. Song, Y.-X. Li, J.-L. Zuo, S. Gao, X.-Z. You, *Eur. J. Inorg. Chem.* **2005**, 766 – 772; c) K. S. Jeong, Y. S. Kim, Y. J. Kim, E. Lee, J. H. Yoon, W. H. Park, Y. W. Park, S.-J. Jeon, Z. H. Kim, J. Kim, N. Jeong, *Angew. Chem.* **2006**, *118*, 8314 – 8318; *Angew. Chem. Int. Ed.* **2006**, *45*, 8134 – 8138.

[9] M. O'Keeffe, *Mater. Res. Bull.* **2006**, *41*, 911 – 915.

[10] a) O. Franke, G. Schuiz-Ekloff, J. Rathousky, J. Starek, A. Zukal, *J. Chem. Soc. Chem. Commun.* **1993**, 724 – 726; b) P. J. Branton, P. G. Hall, K. S. W. Sing, H. Reichert, F. Schüth, K. Unger, *J. Chem. Soc. Faraday Trans.* **1994**, *90*, 2965 – 2967; c) P. I. Ravikovitch, S. C. Ó. Domhnail, A. V. Neimark, F. Schüth, K. K. Unger, *Langmuir* **1995**, *11*, 4765 – 4772; d) M. Kruk, M. Jaroniec, Y. Sakamoto, O. Terasaki, R. Ryoo, C. H. Ko, *J. Phys. Chem. B* **2000**, *104*, 292 – 301.

[11] a) A. Millward, O. M. Yaghi, *J. Am. Chem. Soc.* **2005**, *127*, 17998 – 17999; b) S. Cavenati, C. A. Grande, A. E. Rodrigues, *J. Chem. Eng. Data* **2004**, *49*, 1095 – 1101.

[12] H. Kim, H. Chun, G.-H. Kim, H.-S. Lee, K. Kim, *Chem. Commun.* **2006**, 2759 – 2761.

[13] a) A. T. Armstrong, F. Smith, E. Elder, S. P. McGlynn, *J. Chem. Phys.* **1967**, *46*, 4321 – 4328; b) D. R. Scott, R. S. Becker, *J. Chem. Phys.* **1961**, *35*, 516 – 531.